Characterization of an Independent Structural Unit in Apocytochrome b_5[†]

Cathy D. Moore[‡] and Juliette T. J. Lecomte[*]

Department of Chemistry, The Pennsylvania State University, University Park, Pennsylvania 16802

Received September 10, 1992

ABSTRACT: Apocytochrome b_5 is a partially folded protein which contains a stable structural unit under native conditions [Moore, C. D., Al-Misky, O. N., & Lecomte, J. T. J. (1990) *Biochemistry 30,* 8357–8365]. In this work, the fold of the unit was examined by using ^{1}H and ^{15}N-edited two-dimensional NMR spectroscopy. It was found that it contains four of the five β-strands and two of the six α-helices present in the holoprotein. The remainder of the structure appears to be mostly unstructured and fluctuating among several conformations. The structural unit is stabilized by a hydrophobic core formed by residues from each of the folded elements of secondary structure. Nuclear Overhauser effects and chemical shift values demonstrated that the unit is structurally similar in the apo- and holoproteins. However, the backbone amide hydrogen exchange was found to be much accelerated in the apoprotein. The paramagnetic relaxation agent HyTEMPO was used to probe the packing of the structure. HyTEMPO has unrestricted access to the empty heme binding site whereas it is unable to penetrate the stabilizing core. It was concluded that addition of the heme is necessary for the last strand to dock properly to the rest of the sheet. The kinetics of refolding of the apoprotein were monitored by stopped-flow fluorescence spectroscopy. Extensive protection of the sole tryptophan residue by docking of the two polypeptide termini occurs in less than 60 ms. It was proposed that apocytochrome b_5, with its two-region behavior, might serve as a model for the design of proteins which bind a prosthetic group.

In recent years, considerable progress has been made toward understanding the forces which stabilize the native three-dimensional structure of proteins (Dill, 1990). In parallel efforts, the mechanism of the reaction by which the native fold is achieved from the statistical coil has also been subjected to extensive study. Several models have been proposed which describe the initial step in folding. For example, the framework model involves the formation of secondary structure prior to tertiary structure (Kim & Baldwin, 1982, 1990), and the hydrophobic collapse model favors the rapid reduction of conformational space through hydrophobic interactions (Ptitsyn, 1987; Ptitsyn & Semisotnov, 1992). The forces responsible for attainment and maintenance of organized structure in proteins are difficult to isolate and evaluate. However, in some cases, it is possible to alter the balance of interactions to produce stable states other than the native or fully unfolded states. These alternative states may be related to species fleetingly populated during the folding reaction. Thus, there is much interest in the description of the conformation adopted by proteins under unusual external conditions of pH, salt, and temperature (Kuwajima, 1989). Our approach has been to destabilize the native state not through those means but by the disruption of interactions internal to the native protein, i.e., by the removal of a prosthetic group.

In order to derive valuable information from those altered protein states, structural data are necessary. Destabilized and partially folded species do not lend themselves to traditional X-ray diffraction analysis, and the only method which can yield the desired resolution is nuclear magnetic resonance (NMR)[1] spectroscopy. We are applying NMR spectroscopy to the structural and dynamic characterization of incompletely folded species under native conditions. The system we have chosen is the apoprotein of *b* hemoproteins, and, in this paper, we report on the properties of apocytochrome b_5.

The water-soluble fragment of cytochrome b_5 (cyt b_5) is a small monomeric *b* hemoprotein of known crystal structure (Mathews et al., 1971). Figure 1 presents its ribbon diagram: it contains a five-stranded β-sheet, the central strand lying antiparallel to the other four, and six α-helices. Four of these (helices 2–5) form the heme binding site, and the remaining two (helices 1 and 6, remote from the heme) dock onto the β-sheet. The apoprotein of cyt b_5 (apocyt b_5) contains less repetitive secondary structure and is denatured more readily than the holoprotein (Huntley & Strittmatter, 1972). NMR spectroscopy has demonstrated that apocyt b_5 contains a hydrophobic core including the single tryptophan residue of the water-soluble fragment (Moore & Lecomte, 1990). This core corresponds to a portion of the second hydrophobic core, core 2, described in the crystal structure of the holoprotein (Mathews et al., 1979). A comparison of the properties of the four non-heme-binding histidines in the apo- and holoproteins (Moore et al., 1991) revealed that relative side chain arrangement characteristic of the holoprotein extends beyond the crystallographic boundaries of core 2 into the β-sheet and the N-terminal helix. The C-terminal helix is correctly folded,

[†] Supported by Grant DK 43101 from the National Institutes of Health.

[*] To whom correspondence should be addressed at the Department of Chemistry, The Pennsylvania State University, University Park, PA 16802.

[‡] Current address: Department of Biochemistry, Brandeis University.

[1] Abbreviations: apocyt b_5, apo form of the water-soluble fragment of cytochrome b_5; COSY, two-dimensional correlated spectroscopy; cyt b_5, water-soluble fragment of cytochrome b_5; DQF-COSY, double-quantum-filtered COSY; DIPSI, decoupling in the presence of scalar interactions; DSS, sodium 2,2-dimethyl-2-silapentane-5-sulfonate; holocyt b_5, holoprotein form of the water-soluble fragment of cytochrome b_5; HMQC, heteronuclear multiple-quantum coherence; HSQC, heteronuclear single-quantum coherence; HyTEMPO, 4-hydroxy-2,2,6,6-tetramethylpiperidinyloxy, free radical; INEPT, insensitve nuclei enhanced by polarization transfer; IPTG, isopropyl β-D-thiogalactopyranoside; LB, Luria-Bertani; NMR, nuclear magnetic resonance; NOE, nuclear Overhauser effect; NOESY, two-dimensional nuclear Overhauser spectroscopy; N-t-BOC, *N*-(*tert*-butoxycarbonyl); pH*, pH reading in ^2H_2O solutions, uncorrected for isotope effects; SDS–PAGE, sodium dodecyl sulfate–polyacrylamide gel electrophoresis; TOCSY, total correlation spectroscopy; TPPI, time-proportional phase incrementation.

0006-2960/93/0432-199$04.00/0

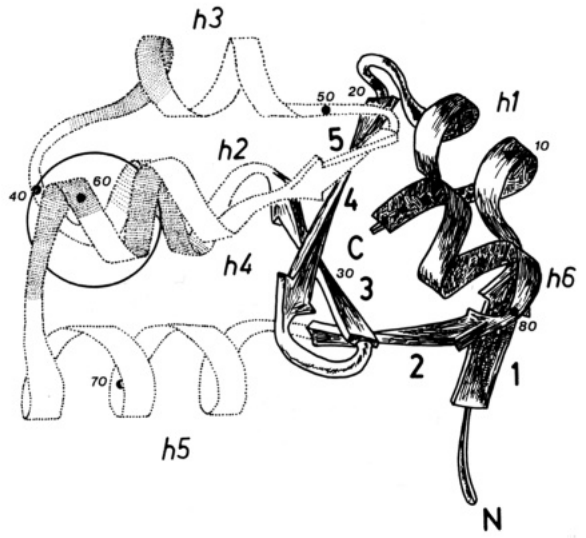

FIGURE 1: Ribbon diagram of holocytochrome b_5 [after Mathews et al. (1971)]. The five strands of the β-sheet are labeled with a single number; the helices are marked as *hn*, where *n* is the helix number; the heme is represented by the open circle. Every tenth residue is indicated with a small filled circle. The ribbon is coded according to the structural properties of the apoprotein discussed in the text. The independent structural unit is illustrated with solid lines; regions whose structure is not well defined are in dotted lines; regions whose structure is similar to that found in the holoprotein, but whose exact position relative to the independent unit was not determined, are stippled.

although in exchange with a small population of alternative conformations (Lecomte & Moore, 1991). These observations led us to propose that the β-sheet and the C- and N-helices form an independent structural unit which provides a scaffold for further folding. Here we pursue the characterization of this unit and study its properties with respect to those in the holoprotein.

Two-dimensional homonuclear and ^{15}N-filtered NMR experiments were performed to secure additional resonance assignments, especially for backbone signals, and to produce a map of the secondary structure. The compactness of hydrophobic core 2 and of the empty heme binding site was probed with the stable radical HyTEMPO (Petros et al., 1990). Amide hydrogen exchange was used as an indicator of the dynamics of the structure. To complete the description, the rate at which the structural unit is formed when the unfolded apoprotein is brought into native conditions was determined by monitoring the change in tryptophan fluorescence intensity as a function of refolding time. All these experiments support a model whereby apocyt b_5 contains two distinct regions: one which folds rapidly and conveys stability; the other which must await the heme to fold and is mainly functional. Apocyt b_5 may be viewed as a protein which has achieved its potentials for folding only locally and for about half the polypeptide chain. Apocyt b_5 provides an opportunity to probe the strongest determinants of structure and stability encoded within the primary structure and eventually to inspect the origins of cooperativity in the folding transition. It may also serve as a guide for the rational design of heme binding sites.

MATERIALS AND METHODS

Materials. The LB broth was prepared with materials from Difco Labs. Antibiotics, M9 supplements, glycerol, and IPTG were purchased from Sigma. Column packing materials were acquired from Bio-Rad and Sigma. Other materials were purchased from various sources: Tris buffer, Sigma or International Biotechnologies Inc; ultrapure urea, Schwarz/Mann Biotechnologies; HyTEMPO, Aldrich; $^{15}NH_4Cl$, Isotech; deuterated solvents, Merck, Sharp, and Dohme Stable Isotopes.

Protein Preparation. The protein used is the water-soluble fragment of rat hepatic cyt b_5 which has been cloned and expressed in *Escherichia coli* (Beck von Bodman et al., 1986). Protein for ^{1}H NMR studies was produced in the TB-1 cell line; an overnight growth in LB broth yielded bright red cells which were harvested by centrifugation. Labeled protein for ^{15}N NMR experiments was produced in strain NCM533, provided by Dr. Richard Shand (University of California at San Francisco). The pUC plasmid carrying the cyt b_5 gene was transformed into the NCM533 strain using the $CaCl_2$ method (Sambrook et al., 1989). The cells were grown in labeled M9-glycerol medium which was supplemented with vitamin B_1 (20 μg/mL), $FeCl_3$ (0.1 mg/mL), and 5-aminolevulinic acid (20 μM), induced with IPTG (500 μM) 4 h after inoculation, and harvested approximately 16 h after induction. The reported method for cell lysis and protein purification was used for both cell lines (Beck von Bodman et al., 1986). Protein purification gave an A_{413}/A_{280} ratio of 5.66 and greater than 5.75 for the unlabeled protein and labeled protein, respectively (Beck von Bodman et al., 1986) and single bands by SDS–PAGE (Laemmli, 1970; Schägger & von Jagow, 1987). The apoprotein was prepared using the acid-butanone method of Teale (1959). Protein concentrations were evaluated by using ϵ_{280} = 10.6 mM^{-1} cm^{-1} for the apoprotein and ϵ_{413} = 114 mM^{-1} cm^{-1} for the oxidized holoprotein (Strittmatter, 1960). Residual holoprotein in apoprotein solutions accounted for less than 1% of the total protein in the unlabeled preparations and for 2.5% of the total protein in the labeled samples.

NMR Samples and NMR Methods. ^{1}H NMR samples were 3–4 mM in both ^2H_2O and ^1H_2O. The ^{15}N NMR sample was approximately 2 mM. The temperature was maintained at 298 K during the experiments unless noted otherwise. The sample for the proton-exchange experiments was prepared by dissolving 16.4 mg of apoprotein lyophilized from ^1H_2O in 400 μL of ^2H_2O at pH* 6.94; a one-dimensional spectrum was acquired within 25 min of the initial addition of ^2H_2O. The apoprotein was dissolved at this pH owing to its limited solubility at pH values below 6.2.

NMR spectra were recorded on a Bruker AM-500 operating in quadrature mode at a proton frequency of 500.13 MHz. DQF-COSY data (Rance et al., 1983) were acquired according to the standard procedure; NOESY (Kumar et al., 1980; Bodenhausen et al., 1984) and TOCSY (Braunschweiler & Ernst, 1983; Rance, 1987) spectra with presaturation of the water were collected with Hahn echo (Davis, 1989), sine modulation in the t_1 domain (Otting et al., 1986), and first-order phase cancellation in ω_1 by t_1 adjustment to compensate for evolution during the preceding and following pulses (Bax & Marion, 1988). In the NOESY experiments, the mixing time τ_m ranged from 10 to 200 ms. The NOESY experiment with τ_m = 50 ms was also recorded with a jump–return observe pulse train (Plateau & Guéron, 1982) to avoid water saturation. TOCSY experiments were recorded with mixing times of 40 and 70 ms using DIPSI-2 pulse train for spin lock (Shaka et al., 1988) with a ca. 45-μs 90° decoupler pulse. Quadrature detection in the ω_1 domain was implemented with the TPPI method (Drobny et al., 1979; Marion & Wüthrich, 1983). Carrier and decoupler frequencies were phase-coherent and placed on the $^1H^2HO$ line in all two-dimensional experiments (Zuiderweg et al., 1986). The transmitter proton 90° was on the order of 7.7 ± 0.2 μs for all experiments. Water elimination

was achieved by presaturation of the resonance with a 1–1.2-s decoupler pulse except in the jump–return experiment.

Acquisition parameters for the ^{1}H NMR experiments were as follows: DQF-COSY data were recorded with a 7042-Hz spectral width in both dimensions using 2K complex points over 512 t_1 increments; Hahn-echo NOESY and TOCSY experiments were acquired over a 12 500-Hz spectral width in ω_2 and 7042 Hz in ω_1 using 4K complex points in t_2 for 460–512 t_1 increments.

The AM-500 NMR spectrometer operates at a 50.68-MHz ^{15}N frequency. Experiments were performed in the inverse mode by detecting proton magnetization. The HSQC and HSQC-NOESY experiments (Bax et al., 1990; Norwood et al., 1990) were recorded with GARP decoupling (Shaka et al., 1985) of the ^{15}N during acquisition; the HSQC-TOCSY experiment utilized DIPSI-2 pulse train (Shaka et al., 1988) for spin locking (τ_m = 40 ms) and no decoupling. No decoupling was used to acquire HMQC data. A 3-ms homospoil pulse with a 10-ms recovery period was applied after the first INEPT sequence to remove any transverse magnetization. The 90° pulse was 25 μs for ^{15}N and 11.1 μs for ^{1}H. The spectral widths for the inverse detected experiments were 7042 Hz in the ω_2 domain and 2747 Hz in the ω_1 domain.

Data were processed on a DEC microVax II using the program FTNMR of Dennis Hare (Research Inc., Woodinville, WA). Resolution enhancement was achieved with a shifted sine bell function, and sensitivity was improved by setting to zero all but the first 800 points in the NOESY and TOCSY transients or all but the first 512 points in the DQF-COSY transients. ^{1}H chemical shifts are referenced to the ^{1}H^{2}HO frequency at 4.76 ppm at 298 K, and ^{15}N shifts are referenced indirectly to ^{15}N-t-BOC-alanine (transmitter frequency of 50.684500 MHz at 120 ppm).

Kinetics of Refolding. Stopped-flow fluorescence data were acquired on a Biologic Stopped-Flow instrument. The protein was excited at 293 nm; all signal below 310 nm was filtered from the observed emission data. A 1.35 mg/mL apoprotein solution was prepared with 5 mM phosphate buffer, pH 6.8, and 8 M urea. Refolding was initiated by rapid 10-fold dilution with buffer and urea to yield a 0.135 mg/mL final protein concentration, and varying final urea concentrations (0.8, 1.0, and 1.25 M). Data were collected in 2-ms intervals (to 2 s) and 0.1-s intervals to 100 s. No further change was observed between 100 and 500 s. The voltages were fitted with the statistical analysis package SAS to a sum of exponentials to yield apparent rate constants and amplitudes of the various kinetic phases. A minimum of three phases was necessary to achieve a good fit.

RESULTS

NMR Spectral Assignments and Secondary Structural Elements. Figure 2 shows the section of a TOCSY spectrum which contains the NH–C$^\alpha$H connectivities. There is extensive overlap in the region comprised within 8.5–8.0 and 4.5–4.0 ppm. Furthermore, a generous count allowing for several instances of complete degeneracy yields less than 75% of the expected cross peaks. This is also the case in DQF-COSY spectra. Both of these problems, overlap and undetectability, have precluded complete assignment of the apocyt b_5 spectrum with two-dimensional homonuclear techniques. In order to improve the resolution and increase the proportion of usable cross peaks, we proceeded with uniform ^{15}N labeling of the protein and collected heteronuclear data sets complementary to the homonuclear ones. Figure 3 shows an ^{1}H–^{15}N HSQC

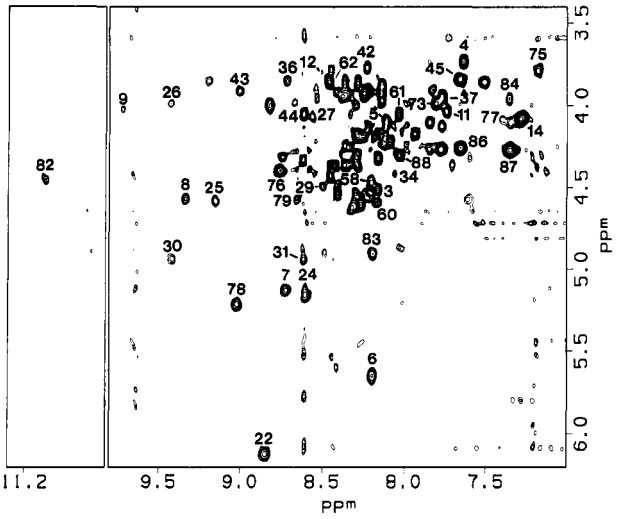

FIGURE 2: Fingerprint region of a TOCSY spectrum recorded at 500 MHz on apocyt b_5 at pH 6.20, 298 K. The spin-locking time was 42 ms. NH–C$^\alpha$H cross peaks are labeled according to their origin as discussed in the text. Note the extensive overlap in the region contained within 8.5–8.0 and 4.5–4.0 ppm.

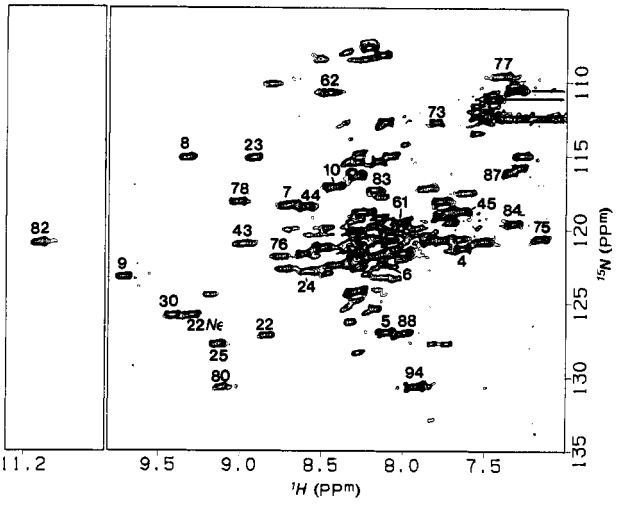

FIGURE 3: Corresponding region of the ^{1}H–^{15}N HSQC spectrum recorded under the conditions described in the legend to Figure 2. ^{15}N–H cross peaks are labeled according to their origin as discussed in the text. The horizontal lines at ^{15}N chemical shifts near 112 ppm and ^{1}H chemical shifts near 7.3 ppm are directed toward the second NH cross peak of Asn and Gln residues (omitted). Note the extensive overlap in the region contained within 8.5–8.0 and 124–118 ppm.

spectrum with the same ω_2 frequency range as in Figure 2. In this case, more than the expected number of cross peaks are counted; in addition, spectral overlap still interferes with complete assignment by two-dimensional methods. Thus, homonuclear and heteronuclear data indicate some unfolding and the existence of multiple conformations.

A few side chain assignments were made recently by comparing apoprotein and reduced holoprotein data and by relying on the model provided by the crystal structure of the oxidized holoprotein. Signals from residues contained in core 2 were recognized (Moore & Lecomte, 1990; Moore et al., 1991), starting with the only tryptophan of the protein (Trp-22) and leading to, among others, Tyr-6, Tyr-7, Val-29, Gly-61, Ile-75, and Ile-76. Helix 6 has also been detected (Lecomte & Moore, 1991) and constitutes the only element of secondary structure previously discussed. Additional assignments are presented below according to the location within the holoprotein (Figure 1; Mathews et al., 1979). Chemical shifts are listed in Table I.

Table I: Rat Liver Apocytochrome b_5 Proton and Nitrogen Resonance Assignments[a]

residue	^{15}N	H^N	H^α	H^β	others
D3	120.6	8.16	4.51	2.48	
V4	121.3	7.63	3.73	1.56	$C^\gamma H_3$ 0.64, 0.29
K5	127.0	8.10	4.10		
Y6	121.9	8.18	5.66	2.83, 2.63	$C^\delta H$ 6.84; $C^\epsilon H$ 6.58
Y7	118.4	8.73	5.13	3.18, 2.45	$C^\delta H$ 6.88; $C^\epsilon H$ 6.54
T8	115.1	9.34	4.58	4.86	$C^\gamma H_3$ 1.19
L9	123.2	9.72	4.02	1.53	$C^\gamma H$ 1.68; $C^\delta H_3$ 0.94, 0.88
E10	117.2	8.42			
E11		7.75	4.02		
I12		8.50	3.79	2.00	$C^\gamma H_3$ 1.03
Q13		8.28			
K14	115.8	7.29	4.09		
H15		7.77			$C^\delta H$ 6.60; $C^\epsilon H$ 8.04
T21			4.68	3.85	$C^\gamma H_3$ 1.14
W22	127.2	8.83	6.14	3.13, 2.87	$^{15}N^\epsilon$ 125.8; $N^\epsilon H$ 9.30; $C^\delta H$ 6.92; $C^{\epsilon 3} H$ 6.72; $C^{\zeta 3} H$ 5.80; $C^\eta H$ 6.42; $C^{\zeta 2} H$ 6.68
V23	115.1	8.92	4.78	1.98	$C^\gamma H_3$ 0.84, 0.77
I24	123.0	8.60	5.16	1.72	$C^\gamma H_3$ 0.81; $C^\gamma H$ 1.75; $C^\delta H_3$ 0.96
L25	127.7	9.14	4.58	1.28, 1.51	$C^\gamma H$ 1.14; $C^\gamma H_3$ 0.60, 0.25
H26		9.43	3.98	3.27	$C^\delta H$ 7.07; $C^\epsilon H$ 8.34
H27		8.56	4.08		$C^\delta H$ 6.91; $C^\epsilon H$ 7.87
K28		8.21	4.78		
V29		8.50	4.50	1.24	$C^\gamma H_3$ 0.66, 0.25
Y30	125.9	9.42	4.93	2.73, 2.26	$C^\delta H$ 6.84; $C^\epsilon H$ 6.68
D31		8.48	4.92	3.14, 2.13	
L32		8.33			
K34		8.06	4.39		
F35		7.74			$C^\delta H$ 6.62; $C^\epsilon H$ 6.88; $C^\zeta H$ 6.80
L36		8.71	3.84		
E37		7.78	3.94		
G42		8.22	3.76		
E43	121.0	9.00	3.91		
E44	118.5	8.61	4.05		
V45	118.8	7.65	3.84	2.06	$C^\gamma H_3$ 0.92, 0.84
N57			4.63		
F58		8.20	4.46	3.08, 2.89	$C^\delta H$, $C^\epsilon H$, $C^\zeta H$ 7.2
D60		8.17	4.59	2.70, 2.59	
V61	119.6	8.03	4.05	2.10	$C^\gamma H_3$s 0.88
G62	110.7	8.46	3.85, 3.85		
H63			4.70	3.28, 3.12	$C^\delta H$ 7.20; $C^\epsilon H$ 8.42
T73	112.8	7.80	3.98	3.90	$C^\gamma H_3$ 0.96
I75	120.6	7.18	3.79	1.56	$C^\gamma H_3$ 0.76; $C^\gamma H$ 1.23; –0.26; $C^\delta H_3$ 0.77
I76	121.9	8.75	4.40	1.61	$C^\gamma H_3$ 0.51; $C^\gamma H$s 0.19; $C^\delta H_3$ –0.96
G77	109.7	7.40	4.32, 4.06		
E78	118.2	9.02	5.21	1.74	
L79		8.72	4.63		$C^\gamma H$ 1.81; $C^\delta H_3$ 1.08, 0.94
H80	130.6	9.11	3.78	2.83, 2.61	$C^\delta H$ 6.98; $C^\epsilon H$ 7.56
D82	121.0	11.07	4.45	2.68, 2.65	
D83	117.4	8.19	4.92	2.67	
R84	119.7	7.30	3.95		
K86		7.66	4.26	2.08	
I87	116.2	7.35	4.26	2.00	$C^\gamma H_3$ 0.92; $C^\gamma H$ 1.45, 1.27; $C^\delta H_3$ 0.89
A88	127.1	8.03	4.23	1.36	
T93		8.15	4.33	4.16	$C^\gamma H_3$ 1.16
L94	130.6	7.93	4.17		$C^\gamma H$ 1.55; $C^\delta H_3$ 0.86, 0.82

[a] Apoprotein chemical shifts are reported at 25 °C, pH 6.20 ■ 0.01. Some of the side chain assignments were previously published under slightly different solvent conditions (Moore & Lecomte, 1990; Moore et al., 1991; Lecomte & Moore, 1991). They are included here for completeness.

(*A*) *Strand 1*: *Residues 3–8*. Figure 4 contains the $C^\alpha H$–NH portion of a 50-ms NOESY spectrum of apocyt b_5 acquired in 90% ^1H_2O/10% ^2H_2O at pH 6.5. NOE cross peaks characteristic of extended chain ($C^\alpha H_i$–NH_{i+1}; Wüthrich, 1986) are expected in this region of the spectrum. The ring protons of Tyr-7 resonating at 6.88 ppm (Moore & Lecomte, 1990) have a strong NOE to a $C^\alpha H$ at 5.13 ppm, which is *J*-connected to two $C^\beta H$s. This set of resonances is attributed to Tyr-7 as well. A TOCSY cross peak between $C^\alpha H$ and an amide proton places the NH of Tyr-7 at 8.73 ppm. These assignments link a known side chain to the backbone and provide a good starting point for further main chain analysis. Connectivities indicative of extended structure continue the chain with NOEs between $C^\alpha H$ and NH of Tyr-7 and Thr-8, and Thr-8 and Leu-9; Leu-9 begins helix 1. *J*-correlated patterns for the respective side chains are consistent with these assignments.

From Tyr-7 toward the N-terminus, Tyr-6 $C^\alpha H$ can be assigned with NOEs to its ring ($C^\delta H$ at 6.84 ppm) and a strong connectivity to Tyr-7 NH. The uniqueness of a successive pair of tyrosines in the primary structure supports the assignments. Severe spectral overlap complicates progression from Tyr-6 NH to Lys-5 $C^\alpha H$, and side chain dipolar contacts were used as well as heteronuclear data. Intense NOEs are observed between the ring of Tyr-6 and both methyl groups of a residue which displays all the TOCSY connectivities of a valine. Assignment to Val-4 is confirmed with Val-4 NH–$C^\alpha H$ NOE to an aspartic acid residue (Asp-3) and Val-4 $C^\alpha H$–NH to a longer side chain (Lys-5). The ^{15}N-edited NOESY spectrum is most helpful for this strand as it

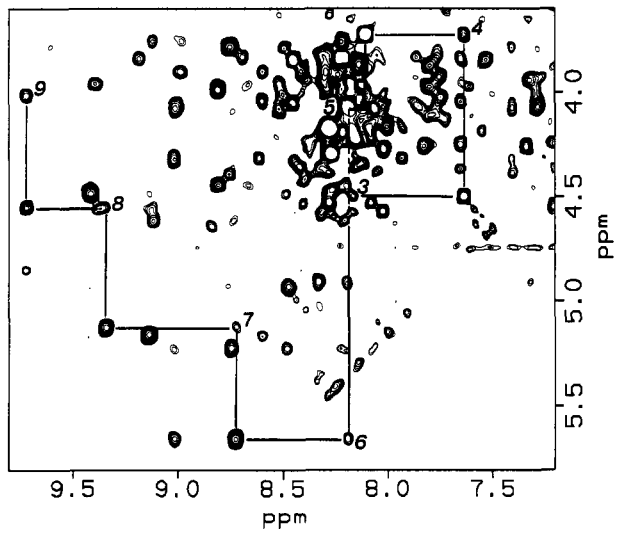

FIGURE 4: $C^{\alpha}H$–NH region of a 50-ms NOESY spectrum recorded on apocyt b_5 in 90% ^1H_2O/10% ^2H_2O at pH 6.5, 298 K. Residues from strand 1 are labeled at their $C^{\alpha}H$–NH cross peak; extended connectivities $C^{\alpha}H_i$–NH_{i+1} are traced from residue 3 to residue 9.

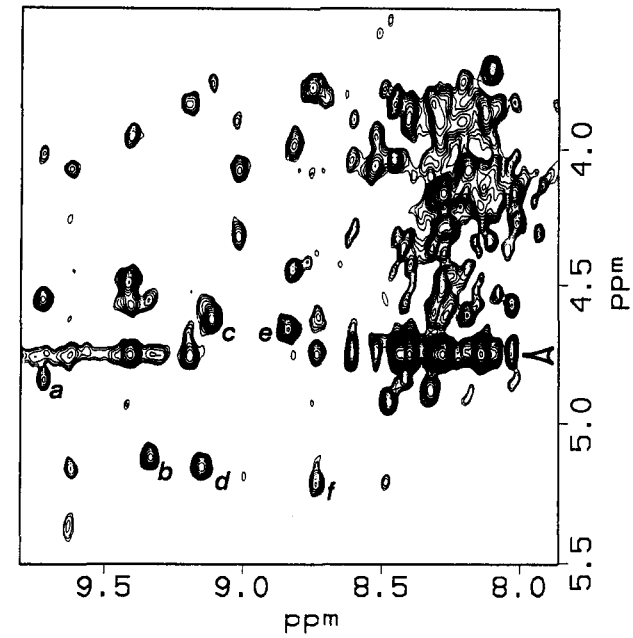

FIGURE 5: $C^{\alpha}H$–NH region of a 50-ms jump–return NOESY spectrum recorded on apocyt b_5 in 90% ^1H_2O/10% ^2H_2O at pH 6.2, 298 K. The NOEs aligned at δ_1 = 4.76 ppm (pointed by the arrow on the right) arise from exchange with the bulk solvent during the mixing time. Other cross peaks are labeled as (a) Thr-8 $C^{\beta}H$ (4.86 ppm) to Leu-9 NH (9.72 ppm), (b) Tyr-7 $C^{\alpha}H$ (5.13 ppm) to Thr-8 NH (9.34 ppm), (c) Leu-79 $C^{\alpha}H$ (4.63 ppm) to His-80 NH (9.11 ppm), (d) Ile-24 $C^{\alpha}H$ (5.16 ppm) to Leu-25 NH (9.14 ppm), (e) Thr-21 $C^{\alpha}H$ (4.68 ppm) to Trp-22 NH (8.83 ppm), (f) Glu-78 $C^{\alpha}H$ (5.21 ppm) to Leu-79 NH (8.72 ppm).

contains all the expected backbone connectivities. Also detected is a connectivity of medium intensity between Asp-3 NH and Val-4 NH which suggests the onset of a turn.

(*B*) *Strand 2*: *Residues 75–79*. The side chain of Ile-76 has been assigned on the basis of its shifted $C^{\delta}H_3$ in both the apo- (–0.96 ppm) and holo- (–1.06 ppm) proteins (Keller & Wüthrich, 1980; Moore & Lecomte, 1990). The shift is due to its position over the ring of Trp-22, and the corresponding NOEs are observed. Ile-76 is the second residue of strand 2; it gives rise to a NH_i–$C^{\alpha}H_{i-1}$ NOE to the previous residue, Ile-75, and $C^{\alpha}H_i$–NH_{i+1} and NH_i–NH_{i+1} NOEs to the one that follows, Gly-77. The presence of both these NOEs implies a bend or kink in the strand; this is consistent with the β-bulge observed in the crystal structure at this position (Mathews et al., 1979). Gly-77 C^{α}Hs are in contact with Glu-78 NH. The $C^{\alpha}H$ of Glu-78 has a strong NOE to the NH of Leu-79, which gives rise to an extended chain connectivity to His-80. The sequential connectivities end at position 80 since residue 81 is a proline.

(*C*) *Strands 4 and 3*: *Residues 21–31*. The first four residues of this segment were assigned primarily through side chain NOEs since many of the C^{α}Hs of interest resonate near the water line. As an example, Thr-21 is readily found in ^2H_2O solutions with $C^{\gamma}H_3$ at 1.12 ppm in dipolar contact with Trp-22 $C^{\alpha}H$ (6.14 ppm). Thr-21 $C^{\alpha}H$ resonates at 4.68 ppm and has an NOE to Trp-22 NH, but the intensity of this effect is inconsistent with extended chain conformation when the solvent transition is saturated. A NOESY data set was recorded with jump–return detection (Plateau & Guéron, 1982) to avoid irradiation at the water frequency. The $C^{\alpha}H$–NH region of the spectrum is presented in Figure 5 where the cross peak between Thr-21 $C^{\alpha}H$ and Trp-22 NH is strong and confirms the presence of the strand.

Trp-22 is the only residue with resolved $C^{\alpha}H$ in this segment of the structure. This $C^{\alpha}H$ has a strong NOE to the NH of the next residue, Val-23, whose $C^{\alpha}H$ resonates under the water line at 4.78 ppm. Val-23 $C^{\alpha}H$ is saturated with the ^1H_2O resonance, and the $C^{\alpha}H$–NH connectivity between it and Ile-24 is therefore not detected. Although the backbone resonances of Ile-24 cannot be directly assigned from Val-23, its $C^{\alpha}H$ can be found through an interstrand NOE to Val-29 $C^{\alpha}H$ (Moore & Lecomte, 1990). Continuation of the $C^{\alpha}H_i$–NH_{i+1} backbone NOEs to a leucine confirms the assignment of Ile-24 $C^{\alpha}H$ and establishes that of Leu-25. Additional connectivities show that the leucine is followed by two histidines, His-26 and His-27 (Moore et al., 1991). The sequence Ile-Leu-His-His is unique within the primary structure and is followed by Lys-Val-Tyr-Asp. All protons of Val-29 are readily assigned through TOCSY connectivities. An extended chain conformation is detected past this residue to Tyr-30 and then to the last residue of strand 3, Asp-31, which shows, in addition to an NH–$C^{\alpha}H$ NOE to Tyr-30, a $C^{\alpha}H$–NH NOE to Leu-32 and a $C^{\alpha}H$–$C^{\alpha}H$ NOE to Trp-22. The NH of Leu-32 also gives rise to a medium-intensity cross peak to Trp-22 $C^{\alpha}H$ and illustrates the close packing of the terminal ends of these two strands.

(*D*) *Strand 5*: *Residues 50–54*. Strand 5 is a short strand of sequence Ala-Gly-Gly-Asp-Ala. The two glycines at positions 51 and 52 have in the holoprotein ^1H and ^{15}N chemical shifts that reflect the proximity of the heme. The apoprotein spectrum displays only two glycines which are shifted from the random coil position: Gly-62 (turn between helices 4 and 5, see below) and Gly-77 (strand 2, see above). The other four have amide protons near 8.3 ppm and amide ^{15}N near 109 ppm (Figure 3). In addition, the ^{15}N–^1H cross peaks observed in the HSQC experiments are broad or doubled. These observations point to conformational multiplicity about an average which lacks organized structure. As a consequence, the resonances from this strand could not be assigned with two-dimensional methods. We also note that the strong NOEs between His-26 and Thr-55, which are observed in the holoprotein (Reid et al., 1987) and manifest docking on the loop between strand 3 and strand 4, are not detected in the absence of the heme.

(*E*) *Helices Remote from the Heme Binding Site*: *Residues 9–15 and 80–89*. $C^{\alpha}H$ of Thr-8, the C-terminal residue of the first strand, is in dipolar contact with the amide proton of

Leu-9, the N-terminal residue of the first helix (Figure 4). From Leu-9, NH_i–NH_{i+1} NOEs indicative of helix 1 can be followed up to residue 15. These NOEs, except the weak 12–13 cross peak, can be seen in Figure 2 of Lecomte and Moore (1991) and are not reproduced here. Further confirmation of helical structure is provided by $C^{\alpha}H_i$–NH_{i+3} contact between Leu-9 and Ile-12. Other intermediate range NOEs between residues 10 and 13, 11 and 14, and 12 and 15 may be present, but spectral overlap precludes unequivocal identification.

Helix 6 is also folded in the apoprotein. Its first residue, His-80, acts as an N-cap (Presta & Rose, 1988). In the apoprotein, the side chain of His-80, and possibly the rest of the helix, is in conformational exchange (Lecomte & Moore, 1991). At pH 6.5 all NH_i–NH_{i+1} connectivities are present except those involving Ser-85. The particular case of residue 85 can be rationalized on the basis of the X-ray structure of the holoprotein: the backbone dihedral angles are irregular and do not provide for an amide hydrogen bond. The N-terminus of helix 6 is docked in its holoprotein location as demonstrated by NOE connectivities between Tyr-7 NH and both His-80 NH and Glu-78 NH.

(F) Heme Binding Site Elements: Residues 34–37, 42–45, and 60–62. NOEs from the ring of Phe-35 are observed to its own amide proton at 7.74 ppm. This proton also has NH_i–$NH_{i\pm1}$ connectivities at 8.06 and 8.71 ppm; the latter proton is in dipolar contact with another NH (7.78 ppm). Although the NH–$C^{\alpha}H$ cross peaks for those amides can be found in correlated data, the side chains are difficult to identify. The TOCSY pattern originating at 7.78 ppm is indicative of a glutamic acid. Phe-35 is preceded by Lys-34 and Thr-33; it is followed by Leu-36 and Glu-37. Thus, we propose tentatively that this short turn of helix belongs to residues 34–37.

A second series of sequential assignments could be made in helix 3; these involve residues 42–45. Val-45 was assigned by default as the last unknown valine residue; its NH has NOEs to both $C^{\alpha}H$ and NH of Glu-44. Residues 42–44 display extended chain connectivities, i.e., Gly-42 $C^{\alpha}H$s give rise to NOEs to Glu-43 NH, and Glu-43 $C^{\alpha}H$ is in dipolar contact with Glu-44 NH. NH–NH NOEs are also detected between residues 44 and 43. All these connectivities are observed in the reduced holoprotein, although the intensities are not identical. The common NOEs imply that the structure at the beginning of helix 3 is similar to that in the holoprotein.

Helix 4 and the turn region connecting it to helix 5 span residues 56–63. Phe-58 shows near degenerate ring signals with few interresidue NOEs at mixing times shorter that 110 ms, but intraresidue NOEs are strong and include the amide proton. Phe-58 NH is in dipolar contact with a $C^{\alpha}H$, not its own, probably belonging to Asn-57. The signals of Glu-59 remain unassigned thus far, and the extended conformation of residues 60–62 has been documented elsewhere (Moore et al., 1991). The subsequent helix found in the holoprotein, helix 5, contains residues 65–71. Residues located in this region of the apoprotein could not been assigned. Past helix 5, Thr-73 is recognized by comparison to holoprotein spectra. Its NH resonates at 7.80 ppm and has a weak NOE to another NH at 7.61 ppm which is in dipolar contact with the ring of Tyr-74 and may belong to it. Lack of resolution, broad lines, and weak NOEs prevent further assignments.

The secondary structure information is summarized in Figure 6 where the arrangement of the β-strands in apocyt b_5 is represented as found in the X-ray structure of the holoprotein (Mathews et al., 1979); the dashed lines denote

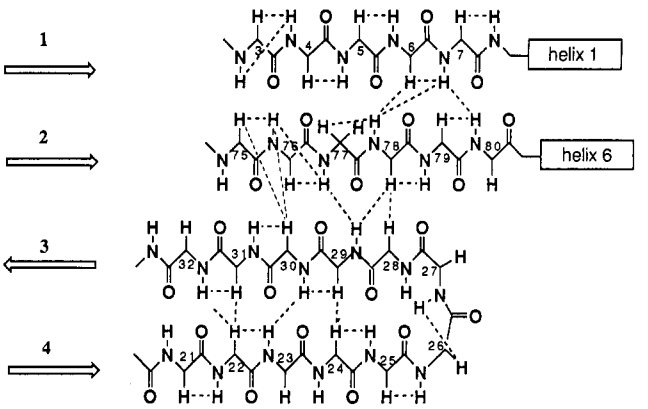

FIGURE 6: β-Sheet of holocytochrome b_5. The diagram is constructed after the refined structure of the beef liver protein (Mathews et al., 1971). The dashed lines denote the NOEs detected in the apoprotein. Strand 5 (residues 50–54) is omitted as it was not identified in the apoprotein spectra.

the backbone NOEs observed in the apoprotein and define the packing of the strands within the sheet. Interstrand NOEs 6 $C^{\alpha}H$–78 NH and 7 NH–80 NH indicate parallel interactions between strands 1 and 2. Strands 4 and 3 give rise to antiparallel $C^{\alpha}H$–$C^{\alpha}H$ connectivities involving residues 22 and 31, and 24 and 29. Antiparallel docking of strand 2 and strand 3 is manifested by other NOEs: 30 $C^{\alpha}H$–75 $C^{\alpha}H$, 30 $C^{\alpha}H$–76 NH, and 29 NH–78 $C^{\alpha}H$. A strong NOE between Glu-78 $C^{\alpha}H$ and a $C^{\alpha}H$ resonating at 4.78 ppm allows for the tentative assignment of Lys-28 $C^{\alpha}H$. These NOEs are all observed in the holoprotein.[2]

The backbone resonances from the independent structural unit are all somewhat displaced from the corresponding signals of the reduced holoprotein. The deviations are smallest (<0.05 ppm) for the residues of strand 1 and largest for those of strands 3 and 4; they reflect the repercussions of heme removal on those elements of structure. In the holoprotein, the hydrophobic side chains of residues 23 and 25 (strand 4) contribute to core 1 and are in van der Waals contact with the prosthetic group. Residues 21 and 24 are close to strand 5. Removal of the heme and release of strand 5 are consistent with the observed shifts. Strand 2 is also affected probably because it follows helix 5 (heme binding site) and leads to helix 6 (fluctuating). Helix 1 presents overall small deviations but larger ones for the residues in contact with those of strand 2. However, even when chemical shift deviations are large, the apoprotein value is not that of the statistical coil (Wishart et al., 1991). The collection of stable secondary structure elements, which constitute the independent structural unit of apocyt b_5, is depicted in Figure 1.

Backbone Amide Hydrogen Exchange. The presence of regular secondary structure is generally associated with retardation of backbone amide hydrogen exchange. In order to examine this effect, a one-dimensional spectrum of the oxidized holoprotein was recorded within 0.5 h after it was dissolved in ^2H_2O at pH 6.8 and room temperature; many NH protons found in the β-sheet persist for several hours after exposure. In contrast, no amide signals were observed in the spectrum of the freshly dissolved apoprotein, even from those residues discussed above which are little affected by heme removal. The jump–return NOESY spectrum (Figure

[2] We have recorded reduced holoprotein spectra and assigned the necessary resonances. Except for occasional discrepancies involving residues in the heme binding site (which are irrelevant for our purposes here), the results are essentially the same as for the calf and pig liver cyt b_5 (Guiles et al., 1990).

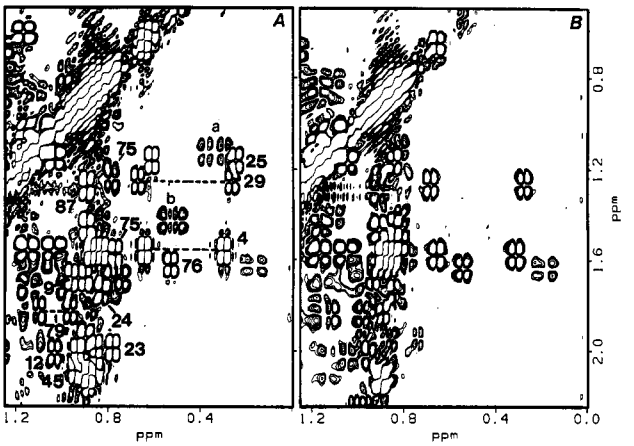

FIGURE 7: Effect of HyTEMPO on apocytochrome b_5 at pH* 6.40, 298 K. (A) Reference DQF-COSY spectrum. (B) DQF-COSY spectrum in the presence of 20 mM HyTEMPO. Some of the assigned methyl groups are marked in the reference spectrum. Cross peaks labeled a and b arise from unassigned leucine residues. Note the complete disappearance of several cross peaks (a, b, Leu-25, Val-45).

5) has cross peaks between the solvent and several amide protons. These cross peaks are due to magnetization transfer either through nuclear Overhauser effect or through exchange with water. The second possibility is the most likely under our experimental conditions, and the jump–return data therefore indicate that several amide hydrogens have a life time shorter than the 50-ms mixing time. The majority of these resonate between 8.0 and 8.6 ppm and are unassigned; they arise from the flexible and unstructured regions of the protein. A few others are known as they occur in the independent structural unit, in particular the NH of His-26 at 9.43 ppm. His-26 gives rise to a strong HSQC ^{15}N–^{1}H connectivity at 125 and 9.5 ppm in the spectra of the holoprotein where protection against exchange is provided by strand 5. In the apoprotein HSQC data, the signal is not observable probably because of fast exchange with bulk solvent and saturation of the proton transition. The accelerated rate is consistent with the structure presented in Figure 1.

HyTEMPO Broadening. The hydrogen exchange experiments suggest that fluctuations of the structure allow access to the solvent even in core 2. The amplitude of the fluctuations can be tested with a molecular probe of size larger than water, for example, the spin label HyTEMPO. HyTEMPO has a stable nitroxide radical which broadens the resonances of the residues that it contacts (Petros et al., 1990). HyTEMPO allows us to determine the relative accessiblity of resolved side chains in the apoprotein.

Two DQF-COSY spectra were recorded, one in the presence of 20 mM HyTEMPO and one in its absence. In this experiment, broadening results in the weakening of cross peaks, sometimes to the point of disappearance. Figure 7 illustrates the effect on the aliphatic region of the apocyt b_5 spectrum. The folded regions of apocyt b_5 described above contain three valines (at positions 4, 23, and 29), four leucines (9, 25, 36, and 79), and five isoleucines (12, 24, 75, 76, and 87). Four residues from core 2, namely, Ile-12, Val-29, Ile-76, and Leu-79, are only slightly affected by the relaxation agent. Other residues in the β-sheet display varying responses. In the first strand, Val-4, Tyr-6, Tyr-7, and Thr-8 appear buried while Leu-9, which belongs to core 2 and is partially accessible in the crystal structure, is broadened more noticeably. Ile-75 (strand 2) is also partially exposed in the solid state and affected by the probe. Three isopropyl groups, from Val-23 (strand 4), Leu-25 (strand 4), and Val-45, belong to hydrophobic

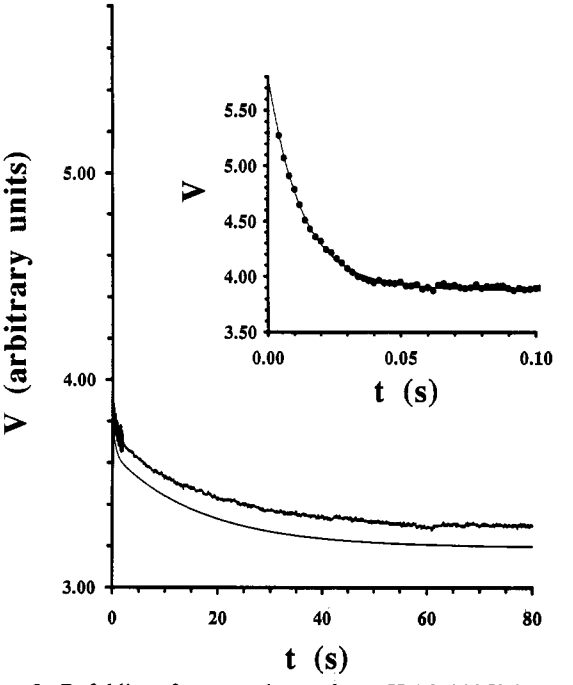

FIGURE 8: Refolding of apocytochrome b_5 at pH 6.8, 298 K, in 5 mM phosphate buffer. The protein was originally unfolded in 8 M urea, and the denaturant was diluted in less than 4 ms to a concentration of 0.8 M. The fluorescence signal (arbitrary voltage units) is plotted versus refolding time. Below the experimental data is drawn a thin line which represents the result of the fit; it is offset by –0.1 unit for clarity. The inset displays the data points over the first 100 ms with a solid line representing the result of the fit. Parameters for the three-phase fit are given in the text.

core 1 and touch the heme group in the holoprotein. They, as well as Phe-58 and Phe-35, are relaxed efficiently by the radical. Also relaxed are two unassigned leucine methyl pairs (a and b in Figure 7), possibly from Leu-32 and Leu-46 (core 1). The control experiment on the holoprotein confirms that the heme provides protection against broadening in core 1. The only affected signals involve the $C^{\beta}Hs$ of Leu-25 as expected from the crystal structure.

HyTEMPO is a small molecule, and all the evidence suggests loosening of the heme binding site. Thus, it may not be surprising that HyTEMPO should access core 1. The advantage of the probe is that it brings to view the segregation of residues in two distinct groups according to their location in the structure. In addition, HyTEMPO is useful in its interaction with specific residues outside the heme binding site. This is best illustrated by Thr-21 and Ile-24, which report on the arrangement of secondary structure elements. In the holoprotein, these residues are buried by the fifth β-strand and the turn leading to it from helix 3; as expected on the base of this structure, broadening of Thr-21 and Ile-24 by the probe is minimal. In contrast, these residues are more accessible in the apoprotein. This is another indication that the turn and the start of the last strand (residues 47–50) are not strongly attached to the rest of the sheet.

Refolding of Urea-Denatured Apocytochrome b_5. To determine how rapidly core 2 is formed when the protein is transferred from highly unfolding conditions (8 M urea) to near-native conditions (ca. 1 M urea), we performed preliminary folding expriments using fluorescence emission to monitor changes in the environment of Trp-22. Typical fluorescence data are shown in Figure 8. The recovery of native signal intensity can be fit with three exponential functions, each with its own amplitude and relaxation rate (Matthews, 1987). The fastest kinetic phase has an apparent

rate constant larger than 70 s^{-1} and accounts for 75% of the signal change. The other two phases have rate constants of ca. 2 s^{-1} (7%) and ca. 0.06 s^{-1} (18%). The three-phase behavior was observed under three distinct final urea concentrations between 0.8 and 1.25 M. No additional information was sought to distinguish between parallel and sequential pathways. Regardless of the mechanism, one can conclude to the rapid development of structure around the single tryptophan.

DISCUSSION

The structure of holocytochrome b_5 consists in three-quarters of a β-barrel flanked by two helices and supporting a small irregular four-helix bundle clamping the heme group in its position. Thus far, the NMR results show that, in the absence of the heme and under native conditions, four out of five strands of the β-structure are arranged as in the holoprotein. The fifth strand, that which closes the bundle, appears not to be docked onto the rest of the structure. Completion of the β-structure by last strand fastening is an event which occurs only upon heme insertion. This model is derived from the chemical shifts of the glycine residues the strand contains, the HyTEMPO effects, and the absence of typical NOEs from the rest of the β-sheet and connecting loops. Weak dipolar contact is observed between residues 25 and 58, away from the docking site. It is possible that hydrophobic interactions in this region are strong enough to direct the last strand in the correct location but not strong enough to maintain a stable hydrogen-bonded network. Computational analysis of Colloc'h and Cohen (1991), examining the residues which terminate the ends of parallel strands, support this assumption. Glycine, of which this short strand has two, has the highest propensity to break β-structure at the C-terminal end of the strand.

Although NOEs characteristic of both α-helices and β-sheet are detected, all amide hydrogens exchange rapidly. Intrinsic exchange rates at pH 7 lie around 15 s^{-1} (Molday et al., 1972). In the apoprotein, the 50-ms jump–return experiment contains amide–water cross peaks substantiating that many amide protons exchange with a rate close or equal to the intrinsic value. By elimination, they belong to the heme binding site. Two mechanisms for hydrogen exchange have been proposed: local unfolding of secondary structure or solvent penetration (Englander & Kallenbach, 1984). It is likely that the first mechanism dominates in the heme binding site. Other amide protons, located in the independent structural unit, yield no cross peak to the water and therefore are marginally protected. An estimate of the protection factor ($k_{exposed}/k_{observed}$) based on the disappearance of all signals in less than 25 min indicates values of 6000 at the highest. This is a lesser degree of protection than observed in apomyoglobin (Hughson et al., 1990).

Stabilization of the unit can be attributed to hydrophobic interactions in core 2. A procedure to detect clusters of side chains densely packed against each other, such as ones which may be integral in protein stability, has been developed by Heringa and Argos (1991). Their algorithm found two clusters in the X-ray structure of oxidized beef liver cyt b_5: one which includes Leu-32, Phe-35, and Phe-74 and a second which contains Tyr-7, Ile-12, Trp-22, Val-29, Asp-31, and Ile-76. This second cluster and core 2 are located in the same region of the structure and overlap in four of the β-strands and the first helix. Dipolar contacts among Trp-22 and the other residues of the cluster are observed in the apoprotein (Moore & Lecomte, 1990; this work). These side chains are located toward the ends of their respective elements of secondary structure and may dictate the collapse of the strands and first helix toward each other.

Fast formation of hydrophobic core 2 is observed by monitoring tryptophan fluorescence during refolding. At least 75% of the protein population conceals the side chain from solvent on a short (<60-ms) time scale. This implies that the two termini find each other quickly. Ubiquitin provides a recently documented example of rapid formation of β-structure. Briggs and Roder (1992) used pulse-labeling techniques to examine secondary structure formation during folding; in this experiment, native hydrogen-bond formation results in NH exchange protection. Most amide sites become 80% protected in 20 ms. Ubiquitin contains a central hydrophobic core surrounded by a five-stranded β-sheet and a single α-helix. Fast-forming hydrogen bonds indicative of tertiary interactions between the helix and the sheet point to the early condensation of the hydrophobic core and may implicate the hydrophobic effect as a driving force for the folding and extreme stability of ubiquitin (Briggs & Roder, 1992). A similar process may be envisioned for apocyt b_5.

The behavior of apocyt b_5 is clearly a consequence of its unique topology. Cytochrome b_{562} is a *b* heme protein of about the same size, folded in a four-helix bundle. The single heme group is positioned between the first and last helices, near the N- and C-termini. It is not deeply buried within the structure, and numerous nonpolar contacts are established among the long four helices. The removal of the heme group yields an apocytochrome which is destabilized but remains almost as folded as the holoprotein (Feng et al., 1991; Feng & Sligar, 1991). In cytochrome b_5 the secondary structural elements which form the binding site do not extend farther than the length of the heme group. Removal of the heme deprives the helices of the majority of stabilizing contacts and exposes nonpolar surface area to solvent. It is possible that the destabilization due to this exposure is compensated by a conformational entropy gain for the structural elements directly in contact with the prosthetic group (Freire & Murphy, 1991) leading to partial unfolding rather than tight collapse. In the case of cytochrome b_5, the unfolding does not propagate to the rest of the structure where the effects are limited to conformational adjustments and increased internal motions. It is conceivable that the exposure of the fourth strand due to the separation of the fith is not sufficient to disrupt the remainder of the β-sheet.

The water-soluble fragment of cytochrome b_5 is a small single-domain protein. Its apoprotein displays structural features which clearly divide it in two distinct regions: a folded entity (residues 3–31 and 75–89) and a largely unfolded section (residues 32–74). This observation matches qualitatively the description offered by Mathews (1985) based on crystal structures and homology in the cytochrome family. According to the analysis of this author, the molecule also contains two entities: the heme binding region, which serves a functional role and extends from residue 21 to 78, and a smaller region (3–20 and 78–87) with a structural (and possibly functional) purpose. The structural region is several residues shorter than detected in the apoprotein. Nevertheless, the fact that two-entity behavior can be presumed from inspection of the holoprotein structure and is confirmed by apoprotein solution studies offers clues for the design of efficient prosthetic group-binding proteins. A possible construct modeled after cytochrome b_5 would include a stable unit, folding autonomously, and a flexible region, which undergoes assisted folding under the action of the prosthetic group. The stable unit would ideally be composed of residues near the N- and C-termini of the protein so that, upon folding, the conformational space available to the rest of the polypeptide chain would be limited.

Adequate side chains would be placed in the connecting loops to provide the environment required for the prosthetic group. As information on other apoproteins becomes available, it will be possible to determine whether this scheme is followed in a significant number of cases.

ACKNOWLEDGMENT

We thank Drs. Shand and Sligar for providing strains and gene, Dr. Chiu for advice on protein production, Dr. Mann and Brian Jones for help with the refolding experiments, Dr. Falzone for assistance in recording heteronuclear data, and Dr. Matthews for critical reading of the manuscript.

REFERENCES

Bax, A., & Marion, D. (1988) *J. Magn. Reson. 78*, 186–191.
Bax, A., Ikura, M., Kay, L. E., Torchia, D. A., & Tschudin, R. (1990) *J. Magn. Reson. 86*, 304–318.
Beck von Bodman, A., Schuler, M. A., Jollie, D. R., & Sligar, S. G. (1986) *Proc. Natl. Acad. Sci. U.S.A. 83*, 9443–9447.
Bodenhausen, G., Kogler, H., & Ernst, R. R. (1984) *J. Magn. Reson. 58*, 370–388.
Braunschweiler, L., & Ernst, R. R. (1983) *J. Magn. Reson. 53*, 521–528.
Briggs, M. S., & Roder, H. (1992) *Proc. Natl. Acad. Sci. U.S.A. 89*, 2017–2021.
Colloc'h, N., & Cohen, F. E. (1991) *J. Mol. Biol. 221*, 603–613.
Davis, D. G. (1989) *J. Magn. Reson. 81*, 603–607.
Dill, K. A. (1990) *Biochemistry 29*, 7133–7154.
Drobny, G., Pines, A., Sinton, S., Weitekamp, D. P., & Wemmer, D. (1979) *Symp. Faraday Soc. 13*, 49–55.
Englander, S. W., & Kallenbach, N. R. (1984) *Q. Rev. Biophys. 16*, 521–655.
Feng, Y., & Sligar, S. G. (1991) *Biochemistry 30*, 10150–10155.
Feng, Y., Wand, A. J., & Sligar, S. G. (1991) *Biochemistry 30*, 7711–7717.
Freire, E., & Murphy, K. P. (1991) *J. Mol. Biol. 222*, 687–698.
Guiles, R. D., Altman, J., Lipka, J. J., Kuntz, I. D., & Waskell, L. (1990) *Biochemistry 29*, 1276–1289.
Heringa, J., & Argos, P. (1991) *J. Mol. Biol. 220*, 151–171.
Hughson, F. M., Wright, P. E., & Baldwin, R. L. (1990) *Science 249*, 1544–1548.
Huntley, T. E., & Strittmatter, P. (1972) *J. Biol. Chem. 247*, 4641–4647.
Keller, R. M., & Wüthrich, K. (1980) *Biochim. Biophys. Acta 621*, 204–217.
Kim, P. S., & Baldwin, R. L. (1982) *Annu. Rev. Biochem. 51*, 459–489.
Kim, P. S., & Baldwin, R. L. (1990) *Annu. Rev. Biochem. 59*, 631–660.
Kumar, A., Ernst, R. R., & Wüthrich, K. (1980) *Biochem. Biophys. Res. Commun. 95*, 1–6.
Kuwajima, K. (1989) *Proteins 6*, 87–103.
Laemmli, U. K. (1970) *Nature* (London) *227*, 680–685.
Lecomte, J. T. J., & Moore, C. D. (1991) *J. Am. Chem. Soc. 113*, 9663–9665.
Marion, D., & Wüthrich, K. (1983) *Biochem. Biophys. Res. Commun. 113*, 967–974.
Mathews, F. S. (1985) *Prog. Biophys. Mol. Biol. 45*, 1–56.
Mathews, F. S., Argos, P., & Levine, M. (1971) *Cold Spring Harbor Symp. Quant. Biol. 36*, 387–395.
Mathews, F. S., Czerwinski, E. W., & Argos, P. (1979) in *The Porphyrins* (Dolphin, D., Ed.) Vol. 7, pp 107–147, Academic Press, New York.
Matthews, C. R. (1987) *Methods Enzymol. 154*, 498–511.
Molday, R. S., Englander, S. W., & Kallen, R. G. (1972) *Biochemistry 11*, 150–158.
Moore, C. D., & Lecomte, J. T. J. (1990) *Biochemistry 29*, 1984–1989.
Moore, C. D., Al-Misky, O. N., & Lecomte, J. T. J. (1991) *Biochemistry 30*, 8357–8365.
Norwood, T. J., Boyd, J., Heritage, J. E., Soffe, N., & Campbell, I. D. (1990) *J. Magn. Reson. 87*, 488–501.
Otting, G., Widmer, H., Wagner, G., & Wüthrich, K. (1986) *J. Magn. Reson. 66*, 187–193.
Petros, A. M., Mueller, L., & Kopple, K. D. (1990) *Biochemistry 29*, 10041–10048.
Plateau, P., & Guéron, M. (1982) *J. Am. Chem. Soc. 104*, 7310–7311.
Presta, L., & Rose, G. D. (1988) *Science 240*, 1632–1641.
Ptitsyn, O. B. (1987) *J. Protein Chem. 6*, 273–293.
Ptitsyn, O. B., & Semisotnov, G. V. (1992) in *Conformations and Forces in Protein Folding* (Nall, B. T., & Dill, K. A., Eds.) Chapter 10, American Association for the Advancement of Science, Washington, D.C.
Rance, M. (1987) *J. Magn. Reson. 74*, 557–564.
Rance, M., Sørensen, O. W., Bodenhausen, G., Wagner, G., Ernst, R. R., & Wüthrich, K. (1983) *Biochem. Biophys. Res. Commun. 117*, 479–485.
Reid, L. S., Gray, H. B., Dalvit, C., Wright, P. E., & Saltman, P. (1987) *Biochemistry 26*, 7102–7107.
Sambrook, J., Fritsch, E. F., & Maniatis, T. (1989) in *Molecular Cloning*, 2nd ed., Cold Spring Harbor Laboratory Press, Cold Spring Harbor, N.Y.
Schägger, H., & von Jagow, G. (1987) *Anal. Biochem. 166*, 368–379.
Shaka, A. J., Barker, P. B., & Freeman, R. (1985) *J. Magn. Reson. 64*, 547–552.
Shaka, A. J., Lee, C., & Pines, A. (1988) *J. Magn. Reson. 77*, 274–293.
Strittmatter, P. (1960) *J. Biol. Chem. 235*, 2492–2497.
Teale, F. W. J. (1959) *Biochim. Biophys. Acta 35*, 543.
Wishart, D. S., Sykes, B. D., & Richards, F. M. (1991) *J. Mol. Biol. 222*, 311–333.
Wüthrich, K. (1986) in *NMR of Proteins and Nucleic Acids*, Wiley, New York.
Zuiderweg, E. R. P., Hallenga, K., & Olejniczak, E. T. (1986) *J. Magn. Reson. 70*, 336–343.